

## Ion Secretion and Isotonic Transport in Frog Skin Glands

H.H. Ussing, F. Lind, E.H. Larsen

August Krogh Institute, The University of Copenhagen, Universitetsparken 13, DK-2100 Copenhagen Ø, Denmark

Received: 30 January 1996/Revised: 12 March 1996

**Abstract.** The aim of this study was to clarify the mechanism of isotonic fluid transport in frog skin glands. Stationary ion secretion by the glands was studied by measuring unidirectional fluxes of  $^{24}\text{Na}^+$ ,  $^{42}\text{K}^+$ , and carrier-free  $^{134}\text{Cs}^+$  in paired frog skins bathed on both sides with Ringer's solution, and with  $10^{-5}$  M noradrenaline on the inside and  $10^{-4}$  M amiloride on the outside. At transepithelial thermodynamic equilibrium conditions, the  $^{134}\text{Cs}^+$  flux ratio,  $J_{\text{Cs}}^{\text{out}}/J_{\text{Cs}}^{\text{in}}$ , varied in seven pairs of preparations from 6 to 36. Since carrier-free  $^{134}\text{Cs}^+$  entering the cells is irreversibly trapped in the cellular compartment (Ussing & Lind, 1996), the transepithelial net flux of  $^{134}\text{Cs}^+$  indicates that a paracellular flow of water is dragging  $^{134}\text{Cs}^+$  in the direction from the serosal- to outside solution. From the measured flux ratios it was calculated that the force driving the secretory flux of  $\text{Cs}^+$  varied from 30 to 61 mV among preparations. In the same experiments unidirectional  $\text{Na}^+$  fluxes were measured as well, and it was found that also  $\text{Na}^+$  was subjected to secretion. The ratio of unidirectional  $\text{Na}^+$  fluxes, however, was significantly smaller than would be predicted if the two ions were both flowing along the paracellular route dragged by the flow of water. This result indicates that  $\text{Na}^+$  and  $\text{Cs}^+$  do not take the same pathway through the glands. The flux ratio of unidirectional  $\text{K}^+$  fluxes indicated active secretion of  $\text{K}^+$ . The time it takes for steady-state  $\text{K}^+$  fluxes to be established was significantly longer than that of the simultaneously measured  $\text{Cs}^+$  fluxes. These results allow the conclusion that — in addition to being transported between cells —  $\text{K}^+$  is submitted to active transport along a cellular pathway. Based on the recirculation theory, we propose a new model which accounts for stationary  $\text{Na}^+$ ,  $\text{K}^+$ ,  $\text{Cl}^-$  and water secretion under thermodynamic equilibrium conditions. The new features of the model, as compared

to the classical Silva-model for the shark-rectal gland, are: (i) the sodium pumps in the activated gland transport  $\text{Na}^+$  into the lateral intercellular space only. (ii) A barrier at the level of the basement membrane prevents the major fraction of  $\text{Na}^+$  entering the lateral space from returning to the serosal bath. Thus,  $\text{Na}^+$  is secreted into the outside bath. It has to be assumed then that the  $\text{Na}^+$  permeability of the basement membrane barrier ( $P_{\text{Na}}^{\text{BM}}$ ) is smaller than the  $\text{Na}^+$  permeability of the junctional membrane ( $P_{\text{Na}}^{\text{JM}}$ ), i.e.,  $P_{\text{Na}}^{\text{JM}}/P_{\text{Na}}^{\text{BM}} > 1$ . The secretory paracellular flow of water further requires that the  $\text{Na}^+$  reflection coefficients ( $\sigma_{\text{Na}}$ ) of the two barriers are governed by the conditions,  $\sigma_{\text{Na}}^{\text{BM}} > 0$ , and  $\sigma_{\text{Na}}^{\text{BM}} > \sigma_{\text{Na}}^{\text{JM}}$ . (iii)  $\text{Na}^+$  channels are located in the apical membrane of the activated gland cells, so that a fraction of the  $\text{Na}^+$  outflux appearing downstream the lateral intercellular space is recirculated by the gland cells. Based on measured unidirectional fluxes, a set of equations is developed from which we estimate the ion fluxes flowing through major pathways during stationary secretion. It is shown that 80% of the sodium ions flowing downstream the lateral intercellular space is recycled by the gland cells. Our calculations also indicate that under the conditions prevailing in the present experiments 1.8 ATP molecule would be hydrolyzed for every  $\text{Na}^+$  secreted to the outside bath.

**Key words:** Exocrine gland — Flux-ratio analysis — Frog skin — Isotonic fluid secretion —  $\text{Na}^+$  recirculation — Paracellular water transport

### Introduction

In a theoretical study on isotonic fluid transport (Ussing & Eskesen, 1989) it was concluded that if the bathing solutions on the two sides of the object are identical, and if there are no electrical potential differences and hydrostatic pressure differences across the object, the active transport of a solute from one side of the object to the

other can never lead to the formation of an isotonic fluid. A driving species always will run ahead of a driven species, whether the driving species is a solute or a solvent. Isotonicity of the transported fluid, however, may be achieved if part of the driving species is returned to the solution of origin. Subsequently, principles of the recirculation theory were illustrated by experiments on secreting frog skin glands (Eskesen & Ussing, 1989) and absorbing toad small intestine (Ussing & Nedergaard, 1993).

Already in 1952 we observed (Koefoed-Johnsen, Ussing & Zerahn, 1952) that frog skin stimulated by application of adrenaline to the inside solution generates a short-circuit current which is no longer carried solely by  $\text{Na}^+$ . A large fraction of the current was carried by a flux of  $\text{Cl}^-$  in the outward direction. We suggested that the skin glands were responsible for the apparently active  $\text{Cl}^-$  transport, but the full understanding of the behavior of  $\text{Cl}^-$  in glands did not emerge until the beautiful Silva-model of the shark rectal gland was proposed (Silva et al., 1977). The rectal gland does not, however, produce an isotonic fluid and the Silva-model cannot, therefore, explain why some glands produce an isotonic solution, while others do not.

The frog skin gland belongs to those producing an isotonic secretion (Watlington & Huf, 1971; Bjerregaard & Nielsen, 1987), and is particularly well suited for the study of this physiological function. The  $\text{Na}^+$  channels of the epidermal cells can be closed with amiloride. If the skin glands are now stimulated, say, by noradrenaline added to the inside solution, after initial stimulation, the skin potential drops and ultimately becomes zero. The disappearance of the skin potential abolishes the  $\text{Cl}^-$  conductance of the epithelial mitochondria-rich cells (Larsen, 1991). Thus, with  $\text{Na}^+$  and  $\text{Cl}^-$  conductance of the surface epithelium both eliminated, and the gland cells fully activated, the transport properties of the skin preparation reflect those of the skin glands. In agreement with this observation, the cAMP-mediated secretory response, evoked by  $\beta$ -adrenergic receptor occupation or by the addition of prostaglandin E<sub>2</sub> to the inside bath, is absent in gland free preparations (Thomson & Mills, 1981, 1983; Bjerregaard & Nielsen, 1987). Following stimulation, electrolyte and water secretions have a dual time course (Bjerregaard & Nielsen, 1987; Eskesen & Ussing, 1989): (i) An initial transient phase with an inside positive electrical potential difference and with the associated short-circuit current containing a significant component carried by the active outflux of  $\text{Cl}^-$ . During this initial secretion phase there is a redistribution of electrolytes and a secretion of mucus, toxins, etc. (ii) Usually, after about one hour the transepithelial potential and, *pari passu*, the short-circuit current vanish and secretion of mucus and other proteins stops. However, for hours the glands continue to produce an isotonic

solution of electrolytes at a constant rate. It is during this stationary secretion phase that our studies of tracer fluxes are being carried out.

With the frog skin preparation we are studying the concerted activity of a large number of small glands comprising acini with very short ducts (Mills & Prum, 1984). Thus, the secretion is as close as one can wish to a primary secretion. Since the acini are small and the macroscopic morphology of glands relatively simple, both forward and backward fluxes of the involved electrolytes can be measured. Thus, we can study secretion with radioactive tracers without perturbing the glands with electrical pulses or by application of drugs. This preparation enables the simultaneous determination of forward and backward fluxes, because the glands of the left and right side of the belly skin of an animal are in the same functional state, for instance, of the moulting cycle<sup>1</sup>.

The purpose of the present study is to examine — in the light of the recirculation theory — the routes in frog skin glands of transepithelial cation fluxes during stationary secretion. We have used  $^{134}\text{Cs}^+$ -tracer fluxes for estimating paracellular transport. This approach is based on the finding that after carrier-free  $^{134}\text{Cs}^+$  is added to the bathing solutions of frog skin it enters the cells via the  $\text{Na}^+/\text{K}^+$ -pump and becomes virtually irreversibly trapped (Ussing & Lind, 1996). Thus, if  $^{134}\text{Cs}^+$  is added to one side of the preparation, the tracer activity recovered from the opposite side can be assumed to have entered this compartment by transport along the high conductance paracellular pathway of the glands. By measuring unidirectional tracer fluxes of  $^{24}\text{Na}^+$  and  $^{42}\text{K}^+$ , respectively, together with unidirectional fluxes of  $^{134}\text{Cs}^+$ , it has been possible to estimate the fraction of the paracellular  $\text{Na}^+$  flux which recirculates via gland cells. Based on such estimates the paper presents a model describing relative ion fluxes through cellular and paracellular pathways. Furthermore, the model accounts for the finding that during stationary secretion, the gland has the capacity to short-circuit itself.

## Materials and Methods

### PREPARATION AND FLUX CHAMBERS

The frogs, *Rana temporaria*, were kept in tap water at 4°C. Whole skin was dissected from double-pithed animals and cut in two symmetrical preparations which were mounted in a flux chamber with an area of 7  $\text{cm}^2$  and with 20 ml of well-stirred outside and inside solutions. The

<sup>1</sup> Slough formation greatly influences all activities of the skin (e.g., Larsen 1971). Skin preparations from the left- and the right hand side of a given animal, however, are always in the same phase of the moulting cycle.

transepithelial potential ( $V_t$ ) of each half skin was continuously monitored via high impedance amplifiers on chart recorders using 0.3 M 3%-agar bridges.  $V_t$  is indicated relative to the grounded outside bath.

## MEASUREMENTS OF FLUXES WITH RADIOACTIVE TRACERS

After isolation and mounting in the flux chambers, the two skin halves were allowed to equilibrate under open-circuit conditions for 30–60 min. Both external and internal solutions were then replaced by fresh Ringer's and  $10^{-4}$  M amiloride was added to the external solutions. After the skin potentials had dropped to near zero mV, noradrenaline was added to the internal bathing solutions at a final concentration of  $10^{-5}$  M. Following another *circa* 60 min of equilibration, external and internal solutions were again replaced by fresh Ringer's containing  $10^{-4}$  M amiloride (external solution) and  $10^{-5}$  M noradrenaline (internal solution), respectively. At this time  $V_t$  was again close to zero mV (e.g., Fig. 1), and radio-isotopes were added. In one series of experiments unidirectional fluxes of  $\text{Na}^+$  and  $\text{Cs}^+$  were studied in the same pair of skins, i.e., influxes of  $^{24}\text{Na}^+$  and  $^{134}\text{Cs}^+$ , respectively, were measured in one of the two half-skins, and outfluxes of  $^{24}\text{Na}^+$  and  $^{134}\text{Cs}^+$ , respectively, were measured in the other of the two half-skins. In another series of experiments unidirectional fluxes of  $\text{K}^+$  and  $\text{Cs}^+$  were studied using a similar protocol. In the cesium/sodium experiments, 40  $\mu\text{l}$  of the  $^{134}\text{Cs}^+$ -stock solution ( $\sim 632$  GBq/g Cs;  $\sim 60$  MBq/ml as carrier-free  $^{134}\text{CsCl}$ ) together with 150  $\mu\text{l}$  of the  $^{24}\text{Na}^+$ -stock solution ( $\sim 10$  GBq/g Na;  $\sim 35$  MBq/ml as NaCl in  $\text{H}_2\text{O}$ ) were added to the 20 ml-external bath of the one half-skin, and to the 20 ml-internal bath of the other. At 10-min intervals, samples of 1,000  $\mu\text{l}$  were withdrawn from the 'cold' solutions and replaced by fresh Ringer's. Simultaneous measurements of unidirectional cesium and potassium fluxes were performed by adding  $^{134}\text{Cs}$  (as above) together with 30  $\mu\text{l}$  of  $^{42}\text{K}^+$  from a stock solution of  $\sim 35$  GBq/g K;  $\sim 212$  MBq/ml as KCl in  $\text{H}_2\text{O}$ .  $^{42}\text{K}^+$  was added in such a way that the final  $\text{K}^+$  concentration in the hot chambers remained 1.88 mM. The radioactivity of samples was counted in a Packard 1900TR Liquid Scintillation Analyzer using the Ultima Gold scintillation cocktail (Packard). Separation of the radioisotopes was achieved by taking advantage of the relatively short half-lives of  $^{24}\text{Na}^+$  (15.0 hr) and  $^{42}\text{K}^+$  (12.5 hr), respectively, as compared to  $^{134}\text{Cs}^+$  (2.1 y). All radioisotopes were purchased from Risø, Roskilde, Denmark.

Fluxes are given as the amount of tracer appearing in 1 ml per 10 min on the *trans* side expressed in *per thousand* (%) of tracer in 1 ml of the bath to which the tracer was added (the *cis* side).

$$J = 1,000 \cdot (\Delta \text{cpm} \cdot \text{ml}^{-1} \cdot 10 \text{ min}^{-1})_{\text{trans side}} / (\text{cpm} \cdot \text{ml}^{-1})_{\text{cis side}}. \quad (1)$$

## SOLUTIONS AND CHEMICALS

In all experiments, Ringer's solutions of similar composition were bathing the outside and the inside of the skin (mM): 113.40  $\text{Na}^+$ , 1.88  $\text{K}^+$ , 1.00  $\text{Ca}^{2+}$ , 114.88  $\text{Cl}^-$ , 2.40  $\text{HCO}_3^-$  with  $\text{pH} = 8.2$  when aerated with atmospheric air. Amiloride was from Merck Sharp & Dohme, and noradrenaline as hydrochloride was from Sigma.

## Results

### FLUXES OF CESIUM AND SODIUM

With identical solutions on the two sides of the skin, addition of amiloride to a final concentration of 100  $\mu\text{M}$

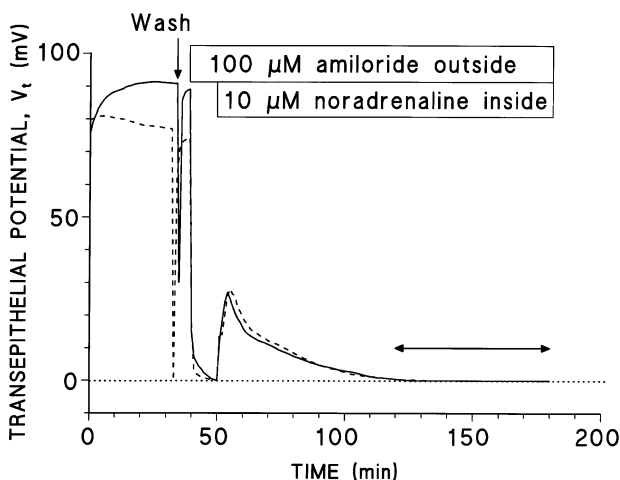


**Fig. 1.** Time course of transepithelial potential ( $V_t$ ) in paired frog skins indicated by continuous and broken line, respectively. After an initial equilibration period, the preparations were exposed to 100  $\mu\text{M}$  amiloride on the outside. During the final period, 100  $\mu\text{M}$  amiloride was present in the outside solutions and 10  $\mu\text{M}$  noradrenaline in the inside solutions. The horizontal arrow indicates the stationary period in which the tracer flux studies were carried out.

in the outside solution resulted in a decrease of the transepithelial potential ( $V_t$ ) to a value close to zero mV. Figure 1 shows that the subsequent application of 10  $\mu\text{M}$  noradrenaline to the serosal bath resulted in a transient stimulation of  $V_t$ . At the new steady state, however, the potential was again very close to zero mV (during the period of flux measurements,  $V_t$  of the two skin halves varied between 1.0 and 0 mV, and 0.7 and 0 mV, respectively). These observations confirm results of a previous study of amiloride-treated short-circuited preparations showing a similar noradrenaline response of the short-circuit current with the steady-state current approaching zero (Eskesen & Ussing, 1989). The time course of tracer appearances on the *trans* side of the preparations, during the stationary period with  $V_t \approx 0$  mV, are presented in Fig. 2. It can be seen that the tracer fluxes are stationary about 20 min after the addition of tracer and that this is independent of whether they are added to the inside or outside bath. The steady-state fluxes of seven experiments carried out with this protocol are shown in Table 1. Directed from the inside bath to the outside bath, in all seven sets of preparations there is a significant net flux of both  $^{24}\text{Na}^+$  and  $^{134}\text{Cs}^+$ . These net fluxes reflect the activity of secretory glands (Bjerregaard & Nielsen, 1987; Eskesen & Ussing, 1989; Ussing & Eskesen, 1989; Nielsen, 1990a,b). With the transepithelial potential difference (and thus the short-circuit current) being practically zero, it follows that if only electrical parameters were measured, the secretory activity of the preparation would have escaped our attention. Bjerregaard and Nielsen (1987) measured — in short-circuited skin of *R. esculenta* — the net fluxes of

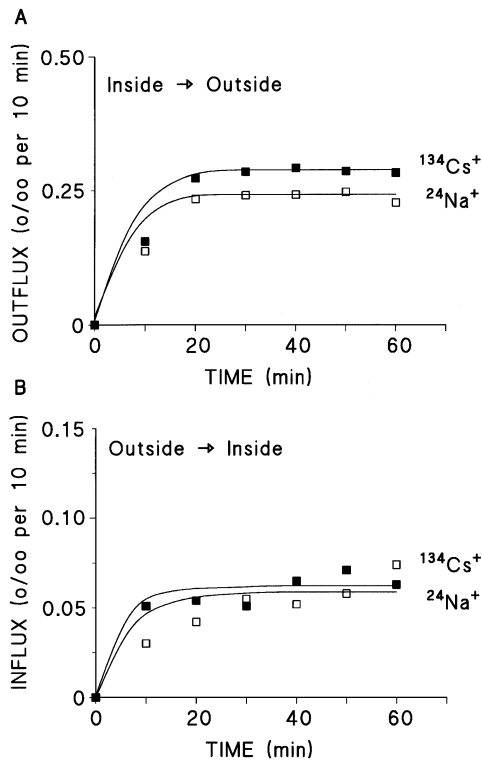


**Fig. 2.** Pre-steady state unidirectional fluxes of  $^{24}\text{Na}^+$  (□) and  $^{134}\text{Cs}^+$  (■) measured during the period indicated by the arrow in Fig. 1. The fluxes were measured simultaneously in two half skins from the same animal. (A) Forward fluxes (secretory direction). (B) Backward fluxes. In both half skins, the tracer appearance per min on the *trans* side of the skin are stationary from about 20 min after the addition of the radioactive tracers to the *cis* side. Although the transepithelial electrochemical potential difference is eliminated (similar ion composition on the two sides,  $V_t = 0$  mV), for both ions at steady state, is the outflux significantly larger than the influx. This finding reveals the secretory activity of the glands.

$\text{Na}^+$ ,  $\text{K}^+$ , and  $\text{Cl}^-$  together with the volume of water secreted and found that the osmolarity of the secreted fluid (232 mOsm) was about the same as that of the Ringer's solution bathing the two sides of the preparation (238 mOsm). The osmolarity of secretions by frog skin *in vivo* was 180 mOsm (Watlington & Huf, 1971).

Because of the irreversible trapping of  $^{134}\text{Cs}^+$  by the epithelial cells (Ussing & Lind, 1996), the transepithelial passage way for radioactive cesium can be considered strictly paracellular. The force ( $F$ ) driving the paracellular flow of tracer  $\text{Cs}^+$  can be estimated from (Ussing, 1952),

$$F = R \cdot T/[F] \cdot \log_e [J_{\text{Cs}}^{\text{out}}/J_{\text{Cs}}^{\text{in}}] \quad (2)$$

With the steady-state  $\text{Cs}^+$  flux ratio varying between 3.25 and 11 ( $J_{\text{Cs}}^{\text{out}}/J_{\text{Cs}}^{\text{in}}$  of Table 1), it is calculated (Eq. 2) that  $F$  varied from 30 to 61 mV. Obviously, however, this force is not electrochemical but reflects solvent drag on

$\text{Cs}^+$ . In other words, the result of this analysis indicates that there is a substantial flow of water between the cells.

The paracellular flow of water is expected also to drag sodium ions along this pathway. It should be possible, then, to estimate the ratio of the  $\text{Na}^+$  fluxes passing together with  $\text{Cs}^+$  along the paracellular route,

$$[J_{\text{Na}}^{\text{out}}/J_{\text{Na}}^{\text{in}}]_{\text{Calculated}} = [J_{\text{Cs}}^{\text{out}}/J_{\text{Cs}}^{\text{in}}]^{1.5} \quad (3)$$

where the exponent (1.5) of the right hand side of Eq. 3 is the ratio of the two ion species' diffusion coefficients in water. The results collected in Table 1 show that the experimental flux ratio in all seven sets of preparations is significantly smaller than the flux ratio calculated by Eq. 3. With the  $\text{Na}^+$  channels in the apical membranes of the epidermal cells blocked by amiloride, the inequality,  $[J_{\text{Na}}^{\text{out}}/J_{\text{Na}}^{\text{in}}]_{\text{Measured}} < [J_{\text{Na}}^{\text{out}}/J_{\text{Na}}^{\text{in}}]_{\text{Calculated}}$ , indicates that  $^{24}\text{Na}^+$  and  $^{134}\text{Cs}^+$  do not follow the same route through the glands. The hypothesis that  $\text{Na}^+$  and  $\text{Cs}^+$  fluxes are flowing via different transepithelial pathways shall be considered in details in the Discussion.

## FLUXES OF CESIUM AND POTASSIUM

With a protocol similar to that used for investigating sodium fluxes, time courses of  $^{42}\text{K}^+$ - and  $^{134}\text{Cs}^+$  fluxes were also studied in paired sets of skin preparations. Results of a single experiment are shown in Fig. 3A and B, and fluxes of nine experiments are listed in Table 2. Also this series of experiments revealed a substantial net flux of tracer- $\text{Cs}^+$  with flux ratios (column 6 of Table 2) spanning a range similar to that indicated in the above studies with sodium (column 8 of Table 1). It can be seen from Fig. 3A and B that it takes somewhat longer for the potassium fluxes to reach steady state, indicating that apart from being transported between cells,  $\text{K}^+$  is submitted to transport along the cellular pathway. By comparing the data presented in Tables 1 and 2, it can also be seen that, contrary to what was found for  $\text{Na}^+$ , the measured  $\text{K}^+$  flux ratio in all nine experiments is substantially larger than the simultaneously measured  $\text{Cs}^+$  flux ratio. With the diffusion coefficient ratio,  $D_{\text{K}}/D_{\text{Cs}} \approx 1$ , and the prevailing transepithelial electrochemical equilibrium conditions, the inequality,  $[J_{\text{K}}^{\text{out}}/J_{\text{K}}^{\text{in}}]_{\text{Measured}} > [J_{\text{Cs}}^{\text{out}}/J_{\text{Cs}}^{\text{in}}]$ , provides the evidence that a component of the outflux of  $\text{K}^+$  is due to active secretion. A contribution of an active pathway, in addition to the paracellular pathway, would account for the above mentioned relatively long pre-steady state period of transepithelial  $^{42}\text{K}^+$ -fluxes.

## Discussion

It seems impossible to reconcile the significant secretion of  $\text{Na}^+$  observed under conditions of eliminated external

**Table 1.** Tracer fluxes of sodium and cesium in frog skin glands ( $J$  in % per 10 min)

Exp.	$J_{Cs}^{out}$	$J_{Cs}^{in}$	$J_{Na}^{out}$	$J_{Na}^{in}$	$J_{Cs}^{out} - J_{Cs}^{in}$	$J_{Na}^{out} - J_{Na}^{in}$	$J_{Cs}^{out}/J_{Cs}^{in}$	$J_{Na}^{out}/J_{Na}^{in}$	$J_{Na}^{out}/J_{Na}^{in}$ Calculated*
13/7	0.65	0.20	0.65	0.20	0.45	0.45	3.25	3.25	5.9
25/7	0.52	0.15	0.40	0.18	0.37	0.22	3.45	2.52	6.4
10/8	0.43	0.11	0.35	0.10	0.32	0.25	3.90	3.50	7.7
19/8	0.28	0.06	0.24	0.06	0.22	0.18	4.73	4.00	10.3
24/8	0.33	0.06	0.28	0.06	0.27	0.22	5.51	4.67	12.9
14/12	0.75	0.093	0.65	0.073	0.66	0.68	8.06	8.9	22.9
15/12	0.44	0.04	0.39	0.04	0.40	0.35	11.0	9.8	36.5

\*  $(J_{Na}^{out}/J_{Na}^{in})_{Calculated} = (J_{Cs}^{out}/J_{Cs}^{in})^{1.5}$

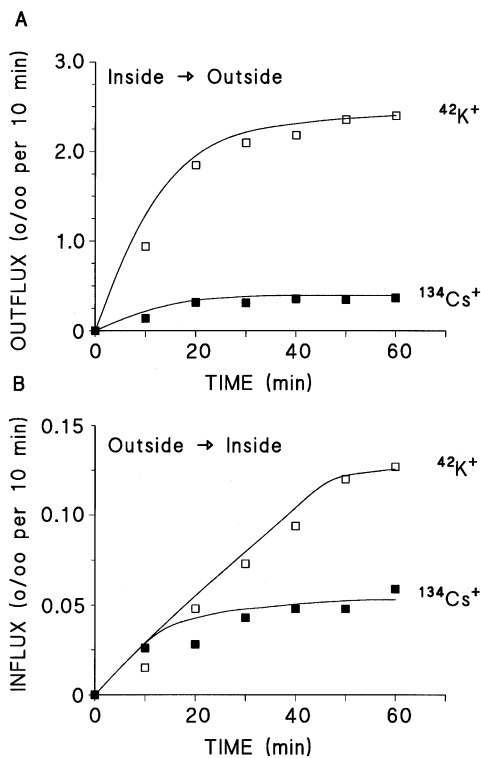


**Fig. 3.** Pre-steady state unidirectional fluxes of  $^{42}\text{K}^+$  (□) and  $^{134}\text{Cs}^+$  (■) measured with a protocol similar to the one indicated in Fig. 2. (A) Forward fluxes (secretory direction). (B) Backward fluxes. For the  $^{42}\text{K}^+$ -fluxes, in both directions are the pre-steady state periods significantly longer than those of the  $^{134}\text{Cs}^+$  fluxes. This indicates a significant contribution from a cellular pathway which is used by  $\text{K}^+$ , but not by  $\text{Cs}^+$ .

transepithelial electrochemical driving forces (Fig. 1; Table 1; Bjerregaard & Nielsen, 1987; Eskesen & Ussing, 1989) with an entirely passive flow of this ion through a low-resistance paracellular pathway as assumed in the Silva-model. However, this model was designed to account for hypertonic NaCl secretion by the shark rectal gland. The frog skin glands and many other exocrine acini secrete an isotonic fluid, and the Silva-model does not deal with this physiological property.

**Table 2.** Potassium and cesium fluxes in frog skin glands ( $J$  in % per 10 min)

Exp.	$J_{Cs}^{out}$	$J_{Cs}^{in}$	$J_{K}^{out}$	$J_{K}^{in}$	$J_{Cs}^{out}/J_{Cs}^{in}$	$J_{K}^{out}/J_{K}^{in}$
16/9	0.366	0.059	2.4	0.13	6.2	18
20/9	0.40	0.055	1.01	0.18	7.2	5.6
23/9	0.44	0.11	2.38	0.25	4.0	9.6
13/10	0.56	0.058	3.00	0.18	9.2	16.2
14/10	0.40	0.065	1.40	0.10	6.1	14.0
3/11	0.34	0.063	1.05	0.07	5.2	15.4
11/11	0.75	0.09	3.6	0.08	8.3	45
14/11	0.54	0.29	1.96	0.25	1.8	7.8
16/11	0.44	0.12	1.8	0.1	3.6	18

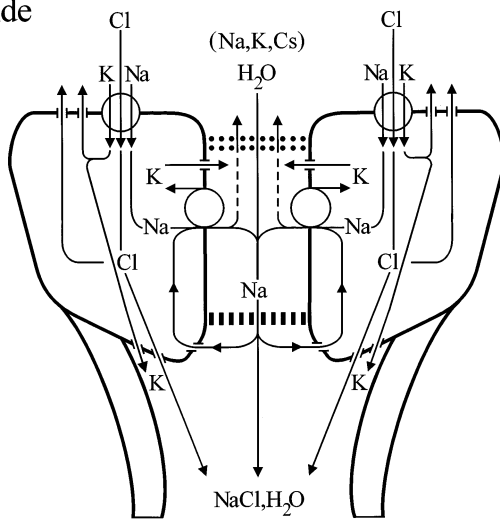
The model of the secreting frog skin gland shown in Fig. 4 has been designed to account for the secretory flux of  $\text{Cl}^-$  and, in addition, the secretory  $\text{Na}^+$ -flux and the associated paracellular water flow under transepithelial thermodynamic equilibrium (short-circuit) conditions. In the remaining part of the paper we shall discuss the new features of this model and compare its properties with the function of the exocrine glands. Finally, we shall discuss the relative contributions of cellular and paracellular pathways for the ion fluxes governing fluid secretion under physiological conditions.

## THE EXOCRINE FROG SKIN GLAND

### *The Cellular Uptake of $\text{Na}^+$ and $\text{Cl}^-$ from the Inside Solution*

Similar to previous models, secretion is driven by a  $\text{Na}^+/\text{K}^+$ -pump creating a steep gradient for  $\text{Na}^+$  that drives the secondary active uptake of  $\text{Cl}^-$  across the basal membrane via coupling to the downhill entrance of  $\text{Na}^+$  (see Fig. 4). The transport system, here assumed to be a  $\{1\text{Na}^+, 2\text{Cl}^-, 1\text{K}^+\}$  cotransporter, is located in the membrane facing the blood side, so the  $\text{Na}^+$  and  $\text{Cl}^-$  transported across the gland epithelium both come from the solution bathing its serosal side. A similar cotransporter

## Inside



## Outside

**Fig. 4.** Model of active frog gland indicating the pathways for the three ions involved in generation of the paracellular fluid flow. Like the Silva-model for NaCl-secretion by shark rectal gland, the active secretion of  $\text{Cl}^-$  is here energized by a  $\text{Na}^+/\text{K}^+$ -ATPase by the coupling of the basal entrance of  $\text{Cl}^-$  to the downhill movement of  $\text{Na}^+$ . The following new features, however, distinguish the frog gland model from the Silva-model: (i) The  $\text{Na}^+/\text{K}^+$  pumps are located in the membrane facing the lateral intercellular space. (ii) A barrier at the level of the basement membrane prevents the major fraction of the pump-generated  $\text{Na}^+$  flux from returning to the serosal bath. Thus, the  $\text{Na}^+$  permeability of the basement membrane ( $P_{\text{Na}}^{\text{BM}}$ ) and of the junctional membrane ( $P_{\text{Na}}^{\text{JM}}$ ) must fulfill the condition,  $P_{\text{Na}}^{\text{JM}} > P_{\text{Na}}^{\text{BM}}$ . Paracellular fluid secretion further requires that the  $\text{Na}^+$  reflection coefficients ( $\sigma_{\text{Na}}$ ) obey the relationships,  $\sigma_{\text{Na}}^{\text{BM}} > 0$ ;  $\sigma_{\text{Na}}^{\text{JM}} > \sigma_{\text{Na}}^{\text{JM}}$ . (iii) The gland cells contain  $\text{Na}^+$  channels in the apical membrane allowing for the recycling of  $\text{Na}^+$ . It should be noted that all of the secreted  $\text{Na}^+$  has passed the cell on its way from the inside solution to the duct lumen. It is also interesting to note that fluid secretion is possible even if  $P_{\text{Na}}^{\text{BM}} = 0$  provided the 'basement membrane' maintains its permeability to water (i.e.,  $\sigma = 1$ ).

was suggested to drive the  $\text{Cl}^-$  uptake by shark gland cells (Hannafin et al., 1983; Greger & Schlatter, 1984a,b), and its presence in frog skin glands was suggested by Mills et al. (1985). They showed that the isoproterenol stimulated  $\text{Cl}^-$  dependent short-circuit current is inhibited by the cotransporter blocker bumetanide added to the serosal bath, and that bumetanide inhibition prevents the gland cell- $[\text{Cl}^-]$  to increase in response to isoproterenol treatment. Thus, there is strong evidence that a  $\{1\text{Na}^+, 2\text{Cl}^-, 1\text{K}^+\}$  cotransporter is present in the serosal membrane of frog gland cells. Generally, however, the basal membrane mechanism could be any combination of transport systems coupling entrance of  $\text{Na}^+$  with entrance of  $\text{Cl}^-$ , e.g., a parallel arrangement of  $\text{Na}^+/\text{H}^+$ -exchange and  $\text{Cl}^-/\text{HCO}_3^-$ -exchange as suggested for salivary glands (Novak & Young, 1986; Melvin, Moran & Turner, 1988; Dissing & Nauntofte, 1990). In the present *in vitro* experiments, however, with an atmospheric  $\text{CO}_2$  tension of the bathing solutions, most likely it is the

cotransport with  $\text{Na}^+$  and  $\text{K}^+$  which dominates the mechanism for cellular  $\text{Cl}^-$  uptake across the basal plasma membrane.

## Chloride Exit Pathways

Similar to the shark rectal gland (Greger et al., 1984; Greger, Schlatter & Gögelein, 1985) the apical exit of  $\text{Cl}^-$  is assumed to take place by diffusion through channels (Fig. 4). *In situ* hybridization, with  $^{35}\text{S}$ -probes generated from the R-domain of *Xenopus* cystic fibrosis transmembrane conductance regulator (CFTR), as well as application of an immunofluorescence technique, with a polyclonal antibody raised against human CFTR, have indicated that CFTR is expressed in gland cells of the skin of *Xenopus laevis* (Engelhardt et al., 1994). Thus, CFTR may constitute the apical chloride conductance in  $\beta$ -adrenergically stimulated gland cells. Furthermore, a recent patch-clamp study of frog gland cells stimulated by cholinergic agonists identified high-conductance  $\text{Cl}^-$  channels in the apical membrane that were activated by membrane depolarization (Andersen & Harvey, 1995). As can be seen in Fig. 4, a fraction of the chloride ions entering the cell via the cotransporter returns to the blood side via channels in the basal membrane. Whole cell and single channel studies of lacrimal glands have identified channels with a high  $\text{Cl}^-$  selectivity in the basal cell membrane which were active during secretion (Marty, Tan & Trautmann, 1984). The return of  $\text{Cl}^-$  to the serosal bath may look like an unnecessary leak of the system. Due to the stoichiometry of the cotransporter and the secretion of a fluid with nearly similar concentrations of  $\text{Na}^+$  and  $\text{Cl}^-$ , however (see also below), the basal  $\text{Cl}^-$  channels constitute a necessary and quantitatively significant exit pathway for  $\text{Cl}^-$ .

## Transport of Sodium

Having entered the gland cell across the basal membrane, sodium ions are pumped out again across the membrane lining the lateral intercellular space. It is a new feature of the model that the  $\text{Na}^+/\text{K}^+$  pumps involved in the secretory state of the gland are assumed located in lateral plasma membranes, only. With this assumption, the gland has the capacity to short-circuit itself and generate a secretory  $\text{Na}^+$  flux under transepithelial thermodynamic equilibrium conditions. However, for  $\text{Na}^+$  to diffuse from the lateral extracellular space into the duct lumen we have further to assume the existence of a paracellular barrier at the level of the basement membrane with a  $\text{Na}^+$  permeability which is significantly smaller than that of the apically located junctional membrane. After passage through the junctional membrane, a fraction of the sodium ions is taken up by the cells again for recirculation. Reuptake of  $\text{Na}^+$  is a prerequisite for the

fluid emerging on the skin surface becoming isotonic (Ussing & Eskesen, 1989). The presence of  $\text{Na}^+$  channels in the apical membrane of the model (Fig. 4) accounts for the reuptake. Mills et al. (1985) found that the intracellular  $[\text{Na}^+]$  in gland cells of frog skin, stimulated for long-time by isoproterenol, was significantly decreased by  $10^{-4}$  M amiloride in the outside bath. This indicates the presence of amiloride-sensitive  $\text{Na}^+$  channels in the apical membrane of activated gland cells. The importance of  $\text{Na}^+$  recirculation, however, calls for further studies of cation transport in this membrane to identify the apical  $\text{Na}^+$  entrance pathway and to study its regulation during transition from the resting to the secreting state of the gland.

### Potassium Exit Pathways

In the steady state there is a continuous flow of potassium ions into the gland cell via the basal cotransporters and the lateral  $\text{Na}^+/\text{K}^+$  pumps. The passive flux of potassium ions from the cell to the surroundings may take one of three pathways (Fig. 4). A major outflux pathway is depicted as  $\text{K}^+$  channels in the lateral membrane of the gland cell. Recycling of  $\text{K}^+$  across this membrane is necessary in order for maintaining continued high activity of the  $\text{Na}^+/\text{K}^+$ -pump.  $\text{K}^+$  channels with this function are most likely located adjacent to the pumps. The basal plasma membrane of the gland cells contains the other significant outflux pathway which has the function of returning the potassium ions entering the cell from the inside bath via the cotransporter. Thus,  $\text{K}^+$  channels in the lateral membrane (facing the intercellular space) and in the basal membrane (facing the blood side) might well constitute different populations. Whole cell and single channel patch-clamp studies have indicated the existence of more than one type of  $\text{K}^+$  channels in exocrine glands (Petersen, 1992). Inward rectifying  $\text{K}^+$ -channels with the specific function of recirculating  $\text{K}^+$  entering the cell via the sodium pump have been characterized in detail in a study of frog epidermis principal cells (Urbach, Van Kerkhove & Harvey, 1994). A recent patch-clamp study of single ion channels identified 'maxi'  $\text{K}^+$  channels in cell-attached patches on the inward-facing membrane of frog skin gland cells (Andersen et al., 1995). These channels were quiescent in the nonstimulated preparation but could be activated by application of muscarinic cholinergic agonists. Activation of muscarinic cholinergic receptors of frog glands evokes the secretory response. However, unlike  $\beta$ -adrenergic receptor activation, occupation of muscarinic receptors results in secretion of only short duration (Schak-Nielsen & Nielsen, 1995). Finally, potassium ions are contained in the secreted fluid (Bjerregaard & Nielsen, 1987), and the flux ratio of this ion indicates active transport in the outward direction (Nielsen & Nielsen, 1994; present study's Table

2). These observations have led to the assumption that the apical membrane contains  $\text{K}^+$  channels which are activated as a result of secretion (Fig. 4). However, due to the relatively low  $[\text{K}^+]$  in the secreted fluid (Bjerregaard & Nielsen, 1987), the outward  $\text{K}^+$  flux through the apical membrane must be small as compared to the  $\text{K}^+$  flux through the  $\text{K}^+$  channels in the basal and lateral membranes, respectively. In connection with this, it is recalled that during stationary secretion the gland short-circuits itself. This condition must be caused by a cellular regulation of the apical and basal membrane conductances leading to identical potentials across apical and basal membranes. Probably, this cannot be accomplished without apical  $\text{K}^+$  channels.

### The Movement of Water

The continuous pumping of sodium across the lateral membrane leads to an accumulation of this ion in the lateral intercellular space and subsequent diffusion to the luminal compartment which — as a result of  $\text{Na}^+$  reuptake across luminal cell membranes — has a somewhat smaller  $[\text{Na}^+]$ . Secretion of water from the serosal bath to the duct lumen requires some additional assumptions. First, as already mentioned above, it is necessary that the basement membrane covering the lateral intercellular space (or another structure with a similar anatomical localization) constitutes a diffusion barrier for sodium, so that this ion preferentially diffuses to the luminal compartment of the duct. This is not identical to claiming that  $\text{Na}^+$  cannot diffuse to the serosal bath. As will be discussed below, a small component of the forward flux of  $^{24}\text{Na}^+$  returns via this pathway to the serosal bath. Both tracer  $\text{Cs}^+$  and tracer  $\text{K}^+$  also exhibit substantial fluxes across this barrier (Table 1, 2, and below). Furthermore, in the studies by Nielsen (1990a) a significant paracellular flow of  $\text{Na}^+$  could be generated by voltage clamping the preparation to  $-100$  mV. Taken together, these observations lead to the conclusion, that the  $\text{Na}^+$  permeability of the inner barrier (at the base of the lateral intercellular space,  $P_{\text{Na}}^{\text{BM}}$ ) and of the apical barrier (the junctional membrane,  $P_{\text{Na}}^{\text{JM}}$ ) are high. However, during secretion they must fulfill the condition,  $P_{\text{Na}}^{\text{JM}} > P_{\text{Na}}^{\text{BM}}$ . Another set of prerequisites for secretory water flow regards the  $\text{Na}^+$  reflection coefficients ( $\sigma_{\text{Na}}$ ) of the two paracellular barriers. With a volume flow in the direction from the blood side to duct lumen, these parameters must be governed by the following inequalities:  $\sigma_{\text{Na}}^{\text{BM}} > 0$ , and  $\sigma_{\text{Na}}^{\text{BM}} > \sigma_{\text{Na}}^{\text{JM}}$ . During stationary secretion it is expected that the lateral membranes facing the paracellular space have no water permeability.

### The Counter Ion for Sodium in the Lateral Space

Following activation of gland cells, sodium ions are pumped into the lateral intercellular space which might

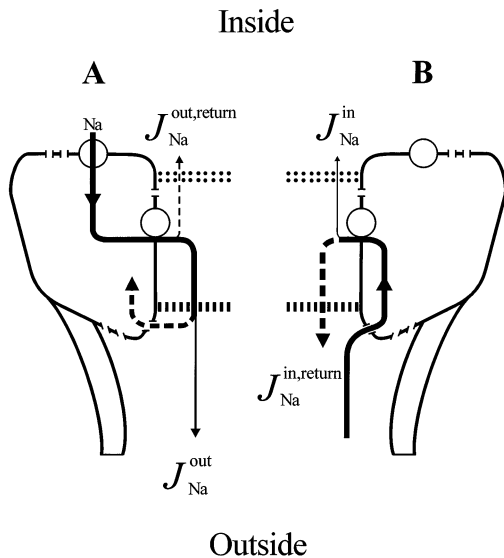


**Fig. 5.** Diagrams indicating pathways for the unidirectional  $^{24}\text{Na}^+$  fluxes. (A) Outflux path. (B) Influx path.  $J_{\text{Na}}^{\text{out}}$  and  $J_{\text{Na}}^{\text{in}}$  are the fluxes which have been measured in the present study. The 'return' fluxes  $J_{\text{Na}}^{\text{out, return}}$  and  $J_{\text{Na}}^{\text{in, return}}$ , are 'invisible' components which can be calculated by the set of equations derived in the text.

expand its volume relative to that of the resting gland. Thus, at the new steady state we expect more  $\text{Na}^+$  in the lateral intercellular space than prior to stimulation. The anion accompanying sodium is most likely chloride. During stationary secretion, the  $\text{Cl}^-$  permeability of the lateral membrane is expected to be negligible. Otherwise there would be a continuous passive flow of  $\text{Cl}^-$  from the cell to the intercellular space. It is more likely that the barrier at the base of the paracellular pathway allows  $\text{Cl}^-$  to exchange between the serosal bath and the lateral space. If this is the case, the junctional membrane's  $\text{Cl}^-$  permeability must be very low because the overall paracellular  $\text{Cl}^-$  conductance of frog skin glands is vanishingly small (Nielsen, 1990a). Thus, during the initial period of accumulation of  $\text{Na}^+$  in the lateral intercellular space, the accompanying  $\text{Cl}^-$  is suggested to be derived from the serosal bath by passive flow through the barrier at the base of the lateral space.

#### ION FLUXES DURING STATIONARY SECRETION

The model shown in Fig. 4 indicates a complicated flow of ions in an exocrine gland during secretory activity. In this section, we apply the measured unidirectional cation fluxes for estimating the quantitative significance of the different ion pathways. In turn, such estimates shall be used in a discussion of the cost of isotonic transport.

#### Sodium Fluxes

Inspection of Fig. 4 shows that a component of the  $^{24}\text{Na}^+$  flux having passed the sodium pump returns via the lat-

eral intercellular space to the compartment of its origin. This is the case whether the unidirectional flux is measured in the forward or in the backward direction. In outflux studies where  $J_{\text{Na}}^{\text{out}}$  is the measured component moving forward into the outside bath, let  $J_{\text{Na}}^{\text{out, return}}$  denote the component returning to the serosal bath (conf. Fig. 5A). In a similar way, in influx studies where  $J_{\text{Na}}^{\text{in}}$  is the measured component flowing into the serosal bath, we let  $J_{\text{Na}}^{\text{in, return}}$  denote the component which is returning to the outside bath (conf. Fig. 5B). We can now set up equations from which the fraction of sodium ions being recirculated can be estimated. The total flux of  $\text{Na}^+$  leaving the lateral intercellular space downstream ( $\sum J_{\text{Na}}^{\text{out, JM}}$ ) is given by,

$$\sum J_{\text{Na}}^{\text{out, JM}} = J_{\text{Na}}^{\text{out}} + J_{\text{Na}}^{\text{in, return}} \quad (4a)$$

while the (relatively small) total flux of  $\text{Na}^+$  crossing the basement membrane barrier in upstream direction ( $\sum J_{\text{Na}}^{\text{in, BM}}$ ) is,

$$\sum J_{\text{Na}}^{\text{in, BM}} = J_{\text{Na}}^{\text{in}} + J_{\text{Na}}^{\text{out, return}} \quad (4b)$$

Since we are dealing with 'appearing fluxes' (Ussing, 1952), only, and in agreement with the assumption discussed above (Eq. 3), we also have,

$$[J_{\text{Na}}^{\text{out}} / J_{\text{Na}}^{\text{out, return}}] = [J_{\text{Cs}}^{\text{out}} / J_{\text{Cs}}^{\text{in}}]^{1.5} \quad (5a)$$

$$[J_{\text{Na}}^{\text{in, return}} / J_{\text{Na}}^{\text{in}}] = [J_{\text{Cs}}^{\text{out}} / J_{\text{Cs}}^{\text{in}}]^{1.5} \quad (5b)$$

This follows from the general principle (Ussing, 1952) that the flux of a substance produced or consumed by a constant source or sink, respectively, in a reversible pathway does not influence the ratio of unidirectional fluxes flowing along the pathway. Thus, from the measured quantities,  $J_{\text{Na}}^{\text{out}}$  and  $J_{\text{Na}}^{\text{in}}$ , together with the ratio of simultaneously measured paracellular unidirectional  $^{134}\text{Cs}^+$  fluxes, the 'return fluxes' can be calculated by Eqs. 5a and b. Then, by the use of Eqs. 4a and b we can calculate the  $\text{Na}^+$  fluxes appearing down and upstream of the lateral space,  $\sum J_{\text{Na}}^{\text{out, JM}}$  and  $\sum J_{\text{Na}}^{\text{in, BM}}$ , respectively. With the measured quantities listed in Table 1, the calculated fluxes are collected in Table 3. It can be seen that, on the average, only one sodium ion out of five is emerging on the outside of the skin while four are submitted to recirculation by gland cells. In other words, 80% of the sodium ions passing down the lateral space originates from the acinar space. The general conclusion is that a very significant fraction of the paracellular  $\text{Na}^+$  flux is recycled.

#### Potassium Fluxes

In principle, it is possible to separate the transepithelial unidirectional  $\text{K}^+$  fluxes in cellular and paracellular com-

**Table 3.** Fluxes of sodium in frog skin glands and estimated fraction of the downstream paracellular  $\text{Na}^+$  flux which is secreted to the outside solution,  $(J_{\text{Na}}^{\text{out}} - J_{\text{Na}}^{\text{in}}) / \sum J_{\text{Na}}^{\text{out}, \text{JM}}$

Exp.	$J_{\text{Na}}^{\text{out}}$	$J_{\text{Na}}^{\text{in}}$	$J_{\text{Na}}^{\text{out,return}}$	$J_{\text{Na}}^{\text{in,return}}$	$\sum J_{\text{Na}}^{\text{out, JM}}$	$\sum J_{\text{Na}}^{\text{in,BM}}$	$\frac{(J_{\text{Na}}^{\text{out}} - J_{\text{Na}}^{\text{in}})}{\sum J_{\text{Na}}^{\text{out, JM}}}$
13/7	0.65	0.20	0.118	1.18	1.83	0.31	0.25
25/7	0.40	0.18	0.062	1.15	1.55	0.24	0.14
10/8	0.35	0.10	0.045	0.77	1.12	0.145	0.22
19/8	0.24	0.06	0.023	0.618	0.858	0.083	0.21
24/8	0.28	0.06	0.021	0.77	1.50	0.081	0.21
14/12	0.65	0.075	0.029	2.10	2.75	0.104	0.21
15/12	0.39	0.04	0.011	1.46	1.85	0.051	0.19
Mean $\pm$ SEM, 0.20 $\pm$ 0.01							

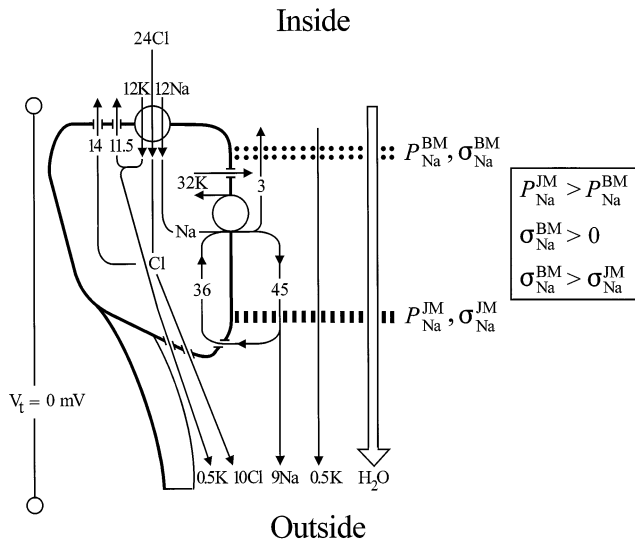


**Fig. 6.** Summary of ion fluxes in a frog skin gland in the stationary secretion phase. The paracellular pathway is permeable to small cations, but not to anions. It is important to note that secretion requires that the  $\text{Na}^+$  permeability of the junctional membrane ( $P_{\text{Na}}^{\text{JM}}$ ) is larger than the  $\text{Na}^+$  permeability of the 'basement' membrane ( $P_{\text{Na}}^{\text{BM}}$ ), and that the  $\text{Na}^+$  reflection coefficients ( $\sigma_{\text{Na}}$ ) of the two membranes obey the inequalities,  $\sigma_{\text{Na}}^{\text{BM}} > 0$  and  $\sigma_{\text{Na}}^{\text{BM}} > \sigma_{\text{Na}}^{\text{JM}}$ . In this presentation it is assumed that the apical  $\text{Na}^+$  channels are so close to the junctional membrane that the associated acinus cells would be able to recirculate the  $\text{Na}^+$  'appearing' at the junctional membrane. In the diagram it is also indicated that the secreting gland short-circuits itself ( $V_t = 0 \text{ mV}$ ).

ponents. The set of equations necessary for performing the calculations would be closely related to that already developed for a similar analysis of  $\text{Na}^+$  and  $\text{Cl}^-$  (Eskesen & Ussing, 1989; Ussing & Nedergaard, 1993), although the special handling of  $\text{K}^+$  by gland cells has to be taken into account. In some skins, however, the paracellular flux amounted to such a small fraction of the total flux that the quantitative separation would have been carried out with a considerable uncertainty. In other experiments, the  $^{42}\text{K}^+$  fluxes did not become truly stationary within the period of observation which, of course, also would introduce errors in the estimates of the two components. Based on less rigorous analysis, it is possible,

however, to discuss the relative contributions of the active and paracellular components to the net flux of  $\text{K}^+$ . Thus, by comparing (Table 2) the flux ratios of  $\text{K}^+$  and  $\text{Cs}^+$ , respectively, it is indicated that in one set of preparations (20/9) the major component was paracellular. In others (e.g., 16/9, 14/11, and 16/11), the active flux through cells must have been, relatively, very significant. There seems to be considerable variation among the different skins, therefore, in the transepithelial active  $\text{K}^+$  flux. Some skins exhibit a relatively very small active secretory  $\text{K}^+$  flux. In such skins, the secreted  $\text{K}^+$  is transported, predominantly, by solvent drag along the paracellular route. In other skins, the paracellular component amounts to a relatively small fraction of the net flux of  $\text{K}^+$ .

### Chloride Fluxes

Since the concentration of  $\text{Na}^+$  and  $\text{Cl}^-$  in the transported fluid is about the same, and all of the secreted sodium ions have been transported to the outside bath via the cotransporter, it follows from the stoichiometry of the cotransporter, that about half of the chloride ions entering the cell via the cotransporter has to return to the serosal bath again.

### Cost of Isotonic Secretion

The diagram of the active frog skin gland shown in Fig. 6 contains net fluxes through the different pathways expressed relatively to one another. The  $\text{Na}^+$  fluxes are derived from numbers given in Table 3. Together with the  $\text{Cl}^-$  fluxes they are considered representative for the type of experiments conducted in the present study. It should be mentioned, however, that there is evidence that the recirculated  $\text{Na}^+$  flux varies with experimental conditions like transepithelial voltage clamping (Ussing & Eskesen, 1989). With respect to  $\text{K}^+$ , as discussed above the active (cellular) component varies considerably among different preparations. The numbers for the  $\text{K}^+$  fluxes in Fig. 6 are in agreement with the finding that the

total net flux of  $K^+$  generally does not exceed 15% of the net flux of  $Cl^-$ .

It can be seen that the ratio between secreted and pumped sodium is 9/(45 + 3). This corresponds to 16 molecules of ATP hydrolyzed for 9 sodium ions secreted. Thus,  $Na^+$  transport by frog skin glands driving secretion of an isotonic fluid between solutions of identical composition is 5–6 times more costly than active transport of  $Na^+$  by frog skin epidermis (Zerahn, 1958), in which any transepithelial water flow depends on a pre established osmotic concentration difference between the bathing solutions.

Thanks are due Mr. Bjarne Brønager for art work. This work was supported by the Alfred Benzon-, Carlsberg-, and Novo-Nordisk Foundations and by the Danish Natural Science Research Council (11-0971).

## References

Andersen, H.K., Harvey, B.J. 1995. Ion channels involved in *in situ* fluid secretion from the frog skin gland. *J. Physiol. London* **482**:24P–25P

Andersen, H.K., Urbach, V., Van Kerkhove, E., Prosser, E., Harvey, B.J. 1995. Maxi  $K^+$  channels in the basolateral membrane of the exocrine frog skin gland regulated by intracellular calcium and pH. *Pfluegers Arch.* **431**:52–65

Bjerregaard, H.F., Nielsen, R. 1987. Prostaglandin  $E_2$ -stimulated glandular ion and water secretion in isolated frog skin (*Rana esculenta*). *J. Membrane Biol.* **97**:9–19

Dissing, S., Nauntofte, B. 1990.  $Na^+$  transport properties of isolated rat parotid acini. *Am. J. Physiol.* **259**:G1044–G1055

Engelhardt, J.F., Smith, S.S., Allen, E., Yankaskas, J.R., Dawson, D.C., Wilson, J.M. 1994. Coupled secretion of chloride and mucus in skin of *Xenopus laevis*: possible role for CFTR. *Am. J. Physiol.* **267**:C491–C500

Eskesen, K., Ussing, H.H. 1989. Transport pathways for  $Na^+$  and  $Br^-$  ( $Cl^-$ ) in noradrenaline-stimulated frog skin (*Rana temporaria*). *Acta Physiol. Scand.* **136**:535–546

Greger, R., Schlatter, E. 1984a. Mechanism of NaCl secretion in the rectal gland of spiny dog fish (*Squalus acanthias*). I. Experiments with isolated *in vitro* perfused rectal gland tubules. *Pfluegers Arch.* **402**:63–75

Greger, R., Schlatter, E. 1984b. Mechanism of NaCl secretion in the rectal gland of spiny dog fish (*Squalus acanthias*). II. Effect of inhibitors. *Pfluegers Arch.* **402**:364–375

Greger, R., Schlatter, E., Gögelein, H. 1985.  $Cl^-$  channels in the apical membrane of the rectal gland “induced” by cAMP. *Pfluegers Arch.* **403**:446–448

Greger, R., Schlatter, E., Wang, F., Forrest, J.N. 1984. Mechanism of NaCl secretion in the rectal gland of spiny dog fish (*Squalus acanthias*). III. Effect of stimulation of secretion by cAMP. *Pfluegers Arch.* **402**:376–384

Hannafin, J., Kinne-Saffran, E., Frieman, D., Kinne, R. 1983. Presence of a sodium-potassium-chloride cotransport system in the rectal gland of *Squalus acanthias*. *J. Membrane Biol.* **75**:73–83

Koefoed-Johnsen, V., Ussing, H.H., Zerahn, K. 1952. Origin of the short-circuit current in the adrenaline-stimulated frog skin. *Acta Physiol. Scand.* **27**:38–48

Larsen, E.H. 1971. The relative contributions of sodium and chloride ions to the conductance of toad skin in relation to shedding of the stratum corneum. *Acta Physiol. Scand.* **81**:254–263

Larsen, E.H. 1991. Chloride transport in high-resistance heterocellular epithelia. *Physiol. Rev.* **71**:235–283

Marty, A., Tan, Y.P., Trautmann, A. 1984. Three types of calcium-dependent channel in rat lacrimal glands. *J. Physiol.* **357**:293–325

Melvin, J.E., Moran, A., Turner, R.J. 1988. The role of  $HCO_3^-$  and  $Na^+/H^+$  exchange in the response of rat parotid acinar cells to muscarinic stimulation. *J. Biol. Chem.* **263**:19564–19569

Mills, J.W., Prum, B.E. 1984. Morphology of the exocrine glands of the frog skin. *Am. J. Anat.* **171**:91–106

Mills, J.W., Thurau, K., Doerge, A., Rick, R. 1985. Electron microprobe analysis of intracellular electrolytes in resting and isoproterenol-stimulated exocrine glands of frog skin. *J. Membrane Biol.* **86**:211–220

Nielsen, R. 1990a. Isotonic secretion via frog skin glands *in vitro*. Water secretion is coupled to the secretion of sodium ions. *Acta Physiol. Scand.* **139**:211–221

Nielsen, R. 1990b. Prostaglandin  $E_2$  enhances the sodium conductance of exocrine glands in isolated frog skin (*Rana esculenta*). *J. Membrane Biol.* **113**:31–38

Nielsen, M.S., Nielsen, R. 1994.  $K^+$  is actively secreted in the frog skin glands. *Acta Physiol. Scand.* **115**:P31

Novak, I., Young, J.A. 1986. Two independent anion transport systems in rabbit mandibular salivary glands. *Pfluegers Arch.* **407**:649–656

Petersen, O.H. 1992. Stimulation-secretion coupling: Cytoplasmic calcium signals and the control of ion channels in exocrine acinar cells. *J. Physiol.* **448**:1–51

Schak-Nielsen, M., Nielsen, R. 1995. Effect of  $Ca^{2+}$  and cAMP on secretion from exocrine glands of frog skin. *Pfluegers Arch.* **S430**:R137, 510

Silva, P., Stoff, J., Field, M., Fine, L., Forrest, J.N., Epstein, F.H. 1977. Mechanism of chloride secretion by shark rectal gland: role of  $Na-K$ -ATPase in chloride transport. *Am. J. Physiol.* **233**:F298–F306

Thomson, I.G., Mills, J.W. 1981. Isoproterenol-induced current in glands of frog skin. *Am. J. Physiol.* **241**:C250–C257

Thomson, I.G., Mills, J.W. 1983. Chloride transport in glands of frog skin. *Am. J. Physiol.* **244**:C221–C226

Urbach, V., Van Kerkhove, E., Harvey, B.J. 1994. Inward-rectifier potassium channels in basolateral membranes of frog skin epithelium. *J. Gen. Physiol.* **103**:583–604

Ussing, H.H. 1952. Some aspects of the application of tracers in permeability studies. *Adv. Enzymol.* **XIII**:21–65

Ussing, H.H., Eskesen, K. 1989. Mechanism of isotonic water transport in glands. *Acta Physiol. Scand.* **136**:443–454

Ussing, H.H., Lind, F. 1996. Trapping of  $^{134}Cs^+$  in frog skin epithelium as a function of short circuit current. *Nephrology (in press)*

Ussing, H.H., Nedergaard, S. 1993. Recycling of electrolytes in small intestine of toad. In: Alfred Benzon Symposium 34: Isotonic Transport in Leaky Epithelia. H.H. Ussing, J. Fischbarg, O. Sten-Knudsen, E.H. Larsen, N.J. Willumsen, editors. pp. 25–34. Munksgaard, Copenhagen

Watlington, C.O., Huf, E.G. 1971.  $\beta$ -Adrenergic stimulation of frog skin mucous glands: Nonspecific inhibition by adrenergic blocking agents. *Comp. Gen. Pharmacol.* **2**:295–305

Zerahn, K. 1958. Oxygen Consumption and Active Sodium Transport in Isolated Amphibian Skin under Varying Experimental Conditions. pp. 1–40. Universitetsforlaget, Aarhus